Available online at www.sciencedirect.com
SCIENCE DIRECT
Journal of Molecular Catalysis A: Chemical 238 (2005) 56–62
JOURNAL OF MOLECULAR CATALYSIS A: CHEMICAL
www.elsevier.com/locate/molcata

# Palladium-platinum powder catalysts manufactured by colloid synthesis I. Preparation and characterization

B. Veisz [a,b], L. Tóth [b], D. Teschner [c,d], Z. Paál [c,*], N. Győrffy [c], U. Wild [d], R. Schlögl [d]

[a] *Department of Colloid Chemistry, University of Szeged, Szeged H-6720, Hungary*
[b] *Research Institute for Technical Physics and Material Science, Hungarian Academy of Sciences, P.O. Box 49, Budapest H-1525, Hungary*
[c] *Institute of Isotopes, CRC, Hungarian Academy of Sciences, P.O. Box 77, Budapest H-1525, Hungary*
[d] *Fritz-Haber-Institut der MPG, Faradayweg 4-6, D-14195 Berlin, Germany*

Received 11 March 2005; accepted 26 April 2005
Available online 15 June 2005

**Abstract**

Palladium, platinum and PdPt bimetallic colloidal particles were prepared in atomic ratios of 4:1, 1:1 and 1:4 by the reduction of $K_2PdCl_4$ and/or $K_2PtCl_4$ in the presence of cationic surfactant, tetradecyltrimethylammonium bromide ($C_{14}$TABr). The nanoparticles in the "as prepared" state were characterized by TEM, EDS and XPS, UPS, permitting to determine their mean particle size, bulk and surface composition. The bulk composition of the bimetallic samples determined by EDS was close to their nominal value, while XPS indicated Pt enrichment near to the surface. All samples in the "as received" state contained surface oxide impurity and contained carbon impurities. The monometallic samples contained considerably more C as the bimetallic ones. A quasi-in situ $H_2$ treatment at 473 K in the electron spectrometer resulted in cleaner metals, containing less carbon and oxygen, as shown by XPS and UPS.
© 2005 Elsevier B.V. All rights reserved.

*Keywords:* Palladium–platinum; Powder catalysts; Colloidal particles

## 1. Introduction

Bimetallic catalysts have been widely used for various catalytic processes [1]. The full understanding of their behaviour needs interdisciplinary knowledge, solid-state physics, alloy theory, chemisorption properties, as summarized concisely in the excellent book by Ponec and Bond [2]. "Electronic" and "ensemble" effects can arise between the components [2,3]. Most of the bimetallic catalysts used in practical applications employ components with rather different catalytic properties [1], like Pt containing less active Sn [4] or more active iridium [5]. Platinum is the best catalyst for "skeletal" reactions of hydrocarbons [2] while palladium is the most widely used catalyst for hydrogenation of unsaturated organic bonds [6–8]. The properties of Pd and Pt in hydrocarbon reactions are otherwise rather close to each other [9–11]. Both are active catalysts, e.g., for opening of small ($C_3$ or $C_4$) cycles [12–14]. The study of their alloy has represented earlier mainly theoretical interest [2]. They have been successfully used, however, for specific purposes, such as sulfur resistant hydrogenation catalysts [15].

Preparation of metal nanoparticles (with a diameter of a few nanometres) has been successfully attempted using methods of colloid chemistry [16]. This is based on reduction of metal salts in the presence of surfactants which then form a surface adlayer preventing the coalescence of small particles, as opposed to "traditional" preparation of metal blacks producing usually larger particles or their aggregates [7,17]. Monometallic Pt and Pd [18,19] as well as PdPt particles [20–22] were synthesized and tested in catalytic reactions [23]. Catalytic tests could be carried out on the nanoparticles alone or deposited on oxide supports, the latter being more suited for practical purposes. These behaved as conventional impregnated catalysts [18,20]. Superior samples were obtained when the synthesis was carried out in the presence of the destined support [23–26].

* Corresponding author. Tel.: +36 1 392 2531; fax: +36 1 392 2533.
*E-mail address:* paal@iserv.iki.kfki.hu (Z. Paál).

1381-1169/$ – see front matter © 2005 Elsevier B.V. All rights reserved.
doi:10.1016/j.molcata.2005.04.064

Pt and Pd forms a solid solution in the whole composition range [2]. Theoretical calculations and analysis indicated more or less inhomogeneous in-depth distribution of the components. Different models applied for their description has been summarized by Ponec and Bond [2]. The theory of metal alloys predicts surface Pd enrichment and was confirmed by Auger electron spectroscopy (AES) of films and powders [27]. This was also observed by Soft X-Ray Emission Spectroscopy of two PdPt foils (containing 15 or 30% palladium) [28]. Pd enrichment was also reported for a disperse PtPd catalyst supported on β-zeolite [29]: its hydrogenation activity increased parallel to the Pd content. Toshima et al. [30], in turn, suggested surface Pt enrichment in PtPd nanoparticles. There are indications of inhomogeneous distribution of Pt and Pd within the small particles [2]: isolated Pt clusters on Pd surface [15] affected the X-ray photoelectron spectroscopic (XPS) signal and could be regarded as indications of Pt enrichment. Adsorption of CO [27] and hydrogen [15] influenced the inhomogeneity. Electron spectroscopy and microscopy showed that the composition for each particle was roughly consistent with that of the parent solution of the Pt and Pd salt [21,22]. The catalytic behaviour in alkane reactions [20], in turn, indicated surface Pd enrichment with some, more active small Pt clusters on the surface. This model was also described by Ponec and Bond [2] and was confirmed by extended X-ray absorption fine structure (EXAFS) analysis, too [31].

The present paper deals with the preparation of PdPt powders of different composition (precipitation in the presence of surfactants), their characterization by photoelectron spectroscopy (XPS, UPS) and electron microscopy (TEM and HRTEM) in the "as prepared state", as well as after reduction. The effect of oxidation–reduction cycles on crystallite sizes, composition as well as their catalytic behaviour in the ring opening reaction of methylethylcyclopropane is going to be reported in a subsequent paper [32].

## 2. Experimental

### 2.1. Materials

Potassium tetrachloropalladate, $K_2PdCl_4$ (98%, Aldrich), potassium tetrachloroplatinate, $K_2PtCl_4$ (99.9+%, Aldrich), tetradecyltrimethylammonium bromide, $C_{14}TABr$ (99%, Aldrich), sodium borohydride, $NaBH_4$ (99%, Aldrich) and 2-propanol (p.a., reanal) were used as received.

### 2.2. Electron microscopy

The size distribution of the particles were determined by transmission electron microscopy in a Philips CM20 analytical TEM. Some samples were studied also in a high resolution microscope, using a JEOL 3010 TEM with a resolving power of 0.17 nm. The bulk composition of the samples were determined by energy dispersive X-ray spectrometry (EDS).

### 2.3. XPS and UPS

Surface composition was determined by X-ray photoelectron spectroscopy (XPS) and ultraviolet photoelectron spectroscopy (UPS). These measurements used a Leybold LHS 12 MCD instrument as described earlier [33,34]; UPS used He II excitation (40.8 eV), pass energy (PE) = 12 eV. A Mg Kα anode was used for XPS (PE = 48 eV). Atomic compositions were determined from peak areas after Shirley (and, in the case of Pd 3d, Bezier type) background subtraction using literature sensitivity factors [35]. This, of course, could not give information on any microscopic inhomogeneity.

## 3. Results and discussion

### 3.1. Catalyst preparation

Nanosized Pd, Pt and PdPt bimetallic particles were prepared by the reduction of $K_2PdCl_4$ (0–3.8 mM) and/or $K_2PtCl_4$ (0–2.8 mM) in the presence of cationic surfactant, $C_{14}TABr$ (19.5 mM). A series of aqueous solutions of the $K_2PdCl_4$, $K_2PtCl_4$ and the $C_{14}TABr$ surfactant were prepared separately and then mixed to give the desired concentrations. The interaction between the precursor metal anions ($PdCl_4^{2-}$, $PtCl_4^{2}$) and the $C_{14}TA^+$ surfactant cation in aqueous solutions results in the formation of organic metal salt [36]. The reaction system was subjected to vigorous stirring when the reducing agent, an aqueous solution of $NaBH_4$, was introduced into the vessel in a 20-fold excess over the precursor metal(s). The reduction was conducted at 323 K. To use the particles as catalysts, the Pd, Pt and PdPt particles were first concentrated via precipitation by the addition of 2-propanol to the parent hydrosol. Washing of the precipitate with ethanol only produced a strongly pyrophoric material. This indicated the extremely high sensitivity of the clusters to atmospheric oxygen and that the nanoscopic character of the primary particles in the precipitate was preserved. The washing was continued by mixing increasing amount of distilled water to the ethanol and finally the precipitate was washed with distilled water only, filtered and stored in closed vessels in air.

The nominal composition of the powders prepared were 100% Pt, 100% Pd and PdPt in the atomic ratio 4:1, 1:1 and 1:4.

### 3.2. Electron microscopy

Typical TEM images of the catalyst powders are shown in Figs. 1–3. Narrow size distribution and a good control of particle size in the range of 6–8 nm in diameter (10 nm average, and up to 15 nm for pure Pt) could be achieved by a systematic variation of the experimental conditions. Most of the particles imaged on the micrographs (Figs. 1–3) exhibited a more or less hexagonal shape projection although some

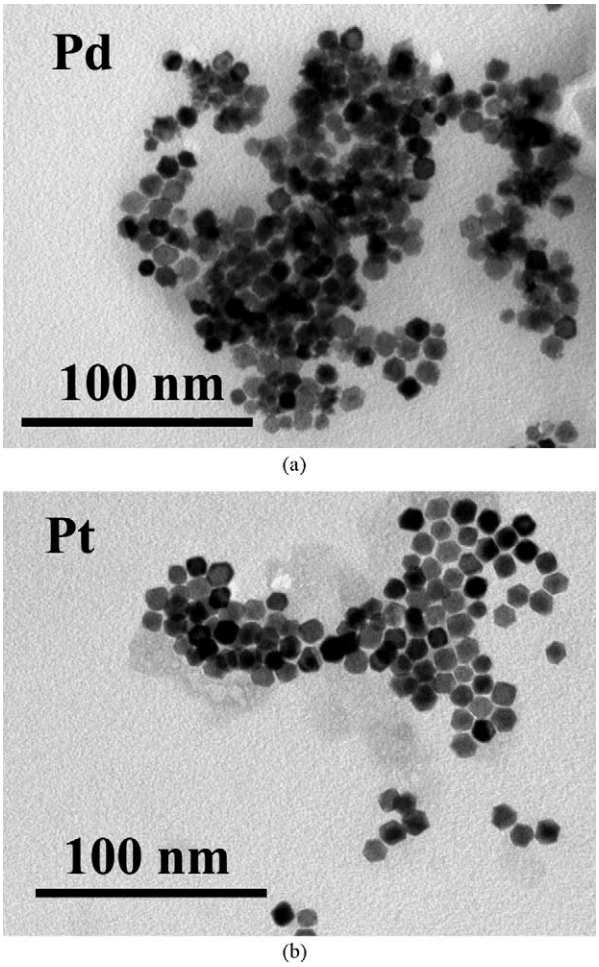


Fig. 1. TEM images of (a) the pure Pd and (b) the pure Pt powders in the "as prepared" state.

quadratic and triangular shapes were occasionally observed, too. In bright-field images, some crystals appear dark and other light due to diffraction contrast: the closer a crystal is to a perfect zone-axis orientation, the more diffracted intensity is excluded from the imaging process, resulting in darker contrast. If a crystal is far from a zone-axis orientation, almost all of the transmitted intensity is within the direct beam, and the crystal is apparently light. The bulk composition of the

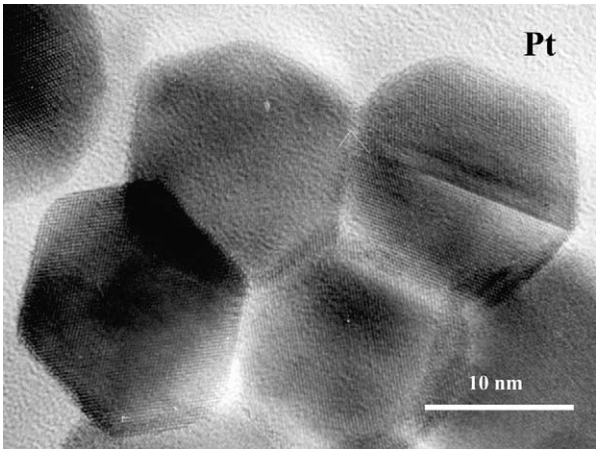


Fig. 2. HRTEM image of the pure Pt powder. The particles exhibited hexagonal shape projection and the crystals were perfectly ordered, except for occasional twinning on (1 1 1) planes.

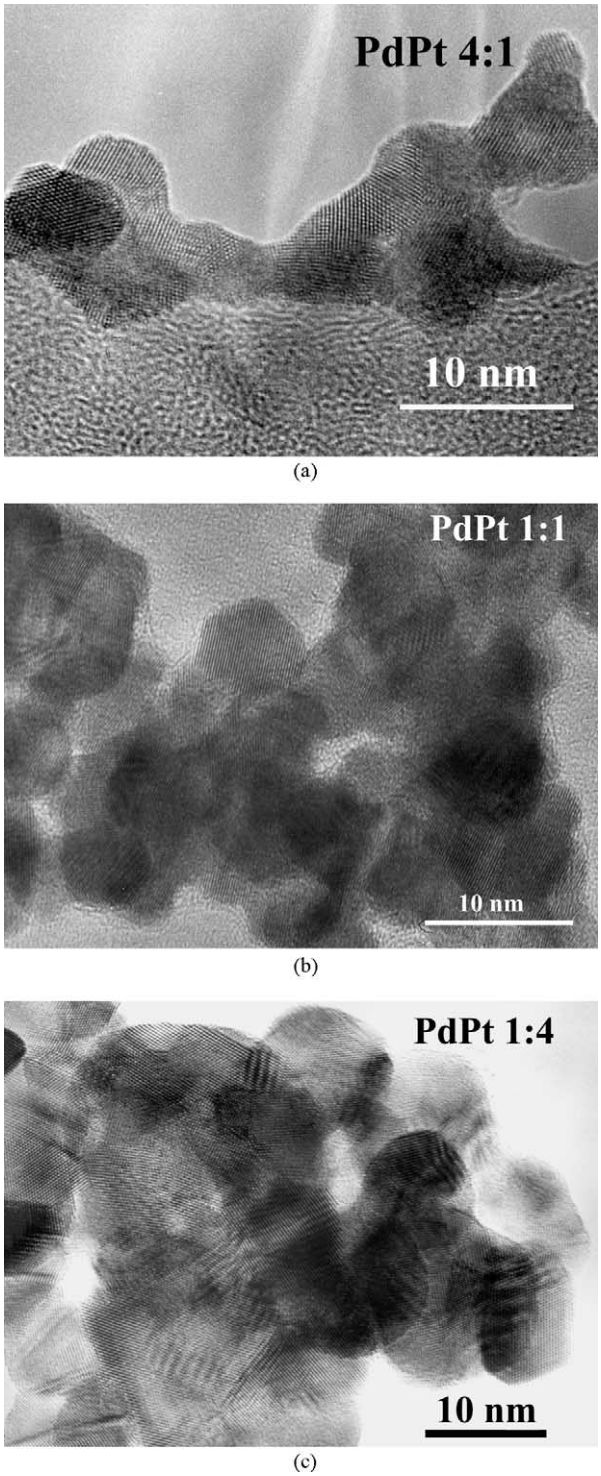


Fig. 3. HRTEM images of (a) the Pd:Pt 4:1, (b) the Pd:Pt 1:1 and (c) the Pd:Pt 1:4 bimetallic catalysts. The alloyed nanoparticles seem to have aggregated and show more irregular, rounded shape than the pure Pd and Pt particles. The amorphous area on the bottom of (a) is the carbon film supporting the metal particles.

Table 1
Comparison of the bulk and the surface Pd:Pt atomic ratio of the PdPt alloy catalysts in the "as received" state and after $H_2$ at 473 K

| Pd:Pt | 1:0 | 4:1 | 1:1 | 1:4 | 0:1 |
|---|---|---|---|---|---|
| Mean particle size, nm (TEM) | 5.5 | 4.2 | 5.8 | 6.5 | 14 |
| Nominal ratio | 100:0 | 80:20 | 50:50 | 20:80 | 0:100 |
| Measured in bulk: EDS | 100:0 | 85:15 | 50:50 | 23:77 | 0:100 |
| Measured at surface: XPS | 100:0 | 73:27 | 28:72 | 7:93 | 0:100 |
| Measured at surface: XPS, after $H_2$ at 473 K | 100:0 | 75:25 | 33:67 | 10:90 | 0:100 |

samples determined by EDS was found to be close to their nominal value (Table 1).

HRTEM of bimetallic nanoparticles (Fig. 3) show more aggregated particles, especially with PdPt 4:1 and 1:4. They showed more irregular, rounded shape than the pure Pt and Pd particles. Individual crystallites of PdPt 1:1 can still be observed (Fig. 3b). Fourier-transform analysis of the local structure in PdPt particles is not possible, due to the very close lattice parameters and identical fcc structure of Pd and Pt.

### 3.3. XPS and UPS

Pt 4f, C 1s, Pd 3d (together with the neighboring Pt 4d), and whenever possible, also the O 1s lines were monitored by XPS. Due to binding energy (BE) coincidence, the Pd 3d spectrum should be separated from the Pt 3p 3/2 peak (done by considerate background subtraction). It was, however, extremely difficult to separate the O 1s line (BE ~ 530–533 eV) from the Pd 3p 3/2 line (BE = 532.5 eV), therefore, the oxygen content was only be determined directly from O 1s, in the pure Pt sample. The O 2p sensitivity is so low that its intensity was below detection limit. Comparing the Pt 4f and Pd 3d lines of the "as received" bimetallic samples with those measured after $H_2$ treatment, a rough estimation could be done concerning their oxidation.

Concentrating on the two main metal components, XPS of the alloy samples indicated more Pt in the "information depth", i.e., near to the surface (Table 1). This finding may be caused by the difference in the reduction rates of the Pd and Pt precursor salts. Accordingly, Pt atoms might have been formed at a slower rate during reduction process and deposited on the surface of Pd particles already formed.

Fig. 4 shows the Pd 3d spectra of untreated catalysts. The BE maximum of the Pd 3d line was at 335.3 eV, like the value measured with another Pd black sample [37]. The peak shapes indicated low amounts of oxidized component(s). The Pt 4f 7/2 peaks show a BE of 71.1 eV, indicating metallic

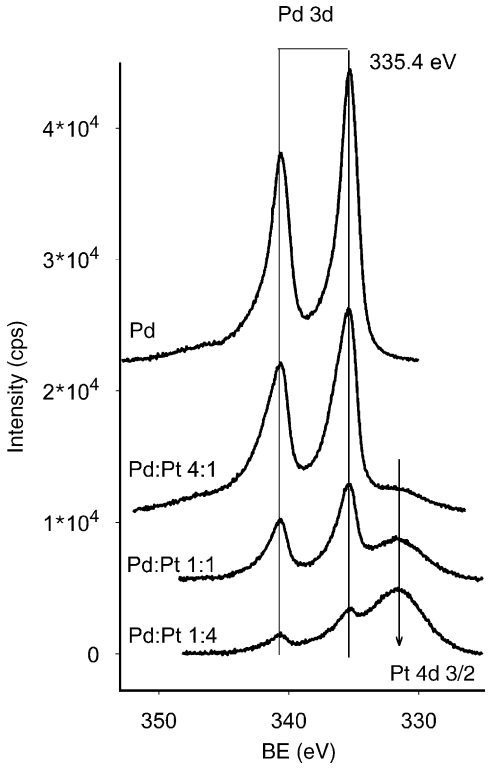


Fig. 4. Pd 3d region of the palladium containing catalysts in the "as received" state.

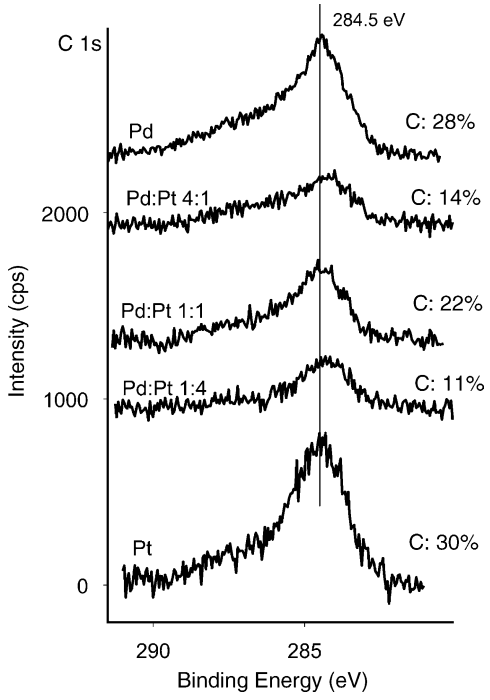


Fig. 5. C 1s XPS spectra for Pt, Pd and mixed PdPt samples in the "as received" state. The carbon percentages are shown on the corresponding spectra.

Table 2
Comparison of the surface composition of the catalysts measured by XPS in the "as is" state and after treatment in $H_2$ at 473 K[a]

| Catalysts | As is (%) | | | | Pretreated in $H_2$ at 473 K (%) | | | |
|---|---|---|---|---|---|---|---|---|
| | Pd | Pt | C | O[a] | Pd | Pt | C | O[a] |
| Pd | 72.1 | 0 | 27.9 | | 75.5 | 0 | 24.5 | |
| PdPt 4:1 | 62.7 | 23.1 | 14.2 | | 67.1 | 21.8 | 11.1 | |
| PdPt 1:1 | 21.7 | 56.5 | 21.8 | | 28.1 | 56.1 | 15.8 | |
| PdPt 1:4 | 5.9 | 83.0 | 11.1 | | 8.9 | 82 | 9.1 | |
| Pt | 0 | 62.8 | 37.2 | | 0 | 68.9 | 31.1 | |
| Pt[b] | 0 | 51.6 | 30.5 | 17.9 | 0 | 61.4 | 27.7 | 10.9 |

[a] The O 1s peak and the Pd 3p 3/2 peaks overlapped, therefore, the O 1s peak could not be determined in Pd containing samples. The composition of those samples was normalized to Pd + Pt + C = 100%.
[b] The composition for all components is shown in the last row.

Pt. The comparison of the C 1s peaks (present as another unavoidable impurity in untreated samples [34,37]) indicates a marked difference between pure metal and alloy particles (Fig. 5). Monometallic Pd and Pt retained more than twice as much carbon as the composite powders. Of the three latter ones, PdPt 4:1 and 1:4 contained conspicuously less carbon. The maximum BE of the C 1s peak (∼284.5 eV) showed that graphitic entities were among the main components, but "$C_xH_y$" and "disordered C" were also present [33,38,39].

Treating the samples with $H_2$ at 473 K represented a customary cleaning process for Pt [34] and Pd [37], although the cleanest metals were observed after a more severe purification process ($O_2$ and $H_2$ treatment [34]). Such results will be reported in Part II [32]. Table 2 indicates that even the present treatment brought the Pd:Pt ratio closer to the nominal values. Up to ∼30% of the original carbon content was removed.

About 60% of the original O 1s area remained on the hydrogen treated Pt sample (Table 2). The degree of oxidation could be judged in other cases from difference spectra before and after $H_2$ treatment. Fig. 6a shows difference spectra for three Pd samples: small maxima appeared in the region corresponding to $Pd^{2+}$ and $Pd^{4+}$ [40]. Similar Pt 4f difference spectra are seen in Fig. 6b for Pt catalysts. The presence of two oxidized Pt species can be seen: the "$PtO_{(ads)}$" entity with

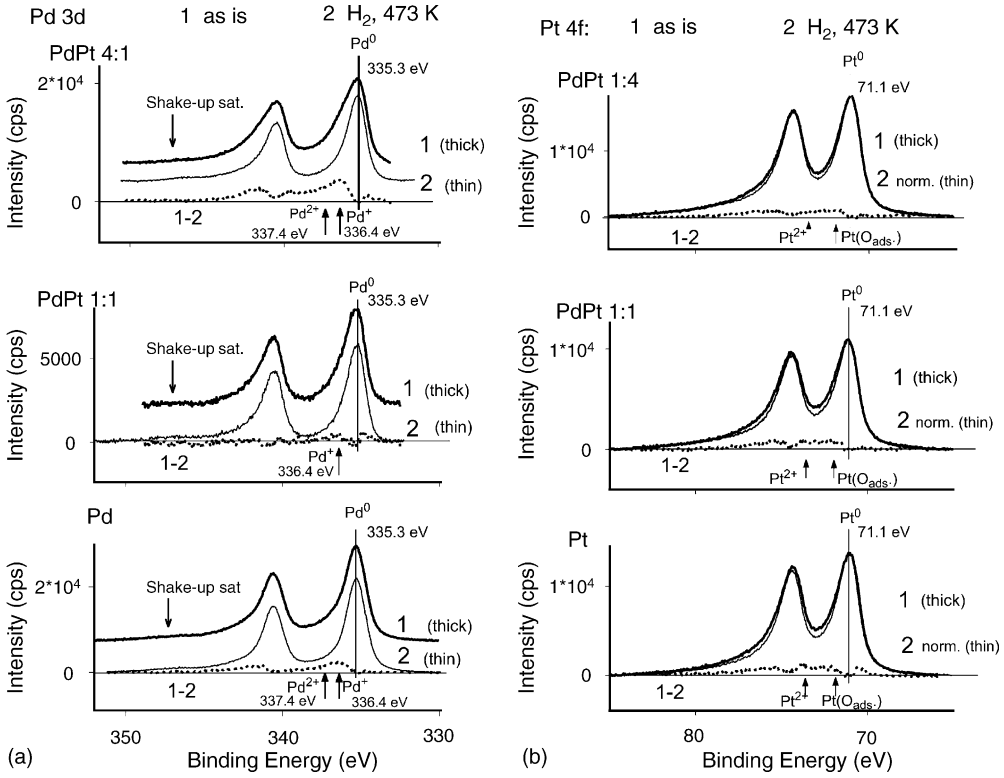


Fig. 6. XP spectra of the main components in the "as received" state and after $H_2$ treatment at 473 K, together with the difference spectra (after normalization for Pt). Monometallic catalysts, 1:1 samples and 4:1 samples (for the richer component) are shown. (a) Pd 3d and (b) Pt 4f.

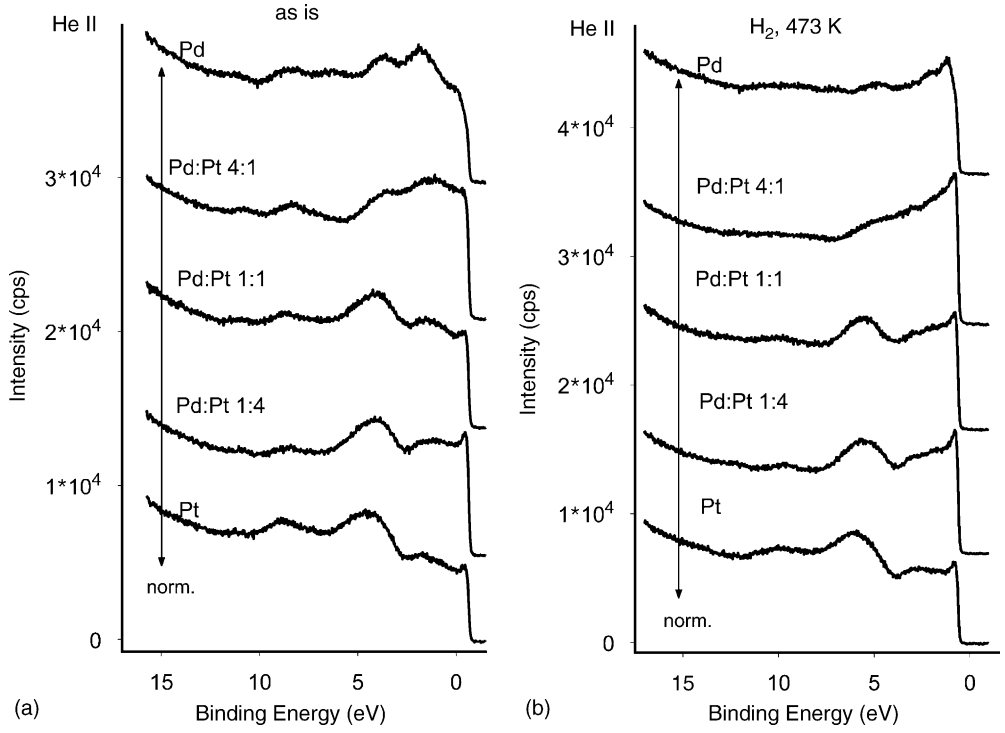


Fig. 7. He II UPS of Pt, Pd and mixed Pt–Pd samples (a) in the "as received" state and (b) after $H_2$ treatment at 473 K.

ΔBE of ∼0.8 eV and the PtO species with ΔBE of ∼2.4 eV [41]. Fig. 6a and b depict also the Pd–Pt 1:1 sample. The Pd 3d peak is shown for Pd–Pt 4:1 and the Pt 4f for Pd–Pt 1:4. The ionic components of Pt are practically the same in all three cases, The Pd–Pt 4:1 sample shows ca. twice as much oxide component than pure Pd.

The O 1s peak of the monometallic Pt sample indicated the presence of four components. These were identified [38] as metal oxide (BE ∼ 530 eV); –OH groups (BE ∼ 531.5 eV), "oxidized carbon" (BE ∼ 532 eV) and adsorbed $H_2O$ (BE ∼ 534 eV). $H_2$ treatment at 473 K removed some O 1s components, the PtO component with lowest BE disappearing entirely.

The general shape of the He II UPS spectra is seen in Fig. 7. The Fermi-edge (FE) intensity of the untreated samples was lowest in the monometallic samples, in agreement with their large carbon impurity. Oxygen has also been detected on Pt, although the Pt 4f spectrum showed minor amounts of "oxidized Pt", in agreement with the O 1s peak. More surface OH and $H_2O$ can be assumed (broadening at ca. 6 eV and a peak at >10 eV [37,38]). The He II UP spectrum of Pd-rich samples showed a cleaner metal state after hydrogen treatment (more intense Fermi-edge and the disappearance of the O 2p binding orbitals at ∼2 and ∼4 eV). The carbon component never formed a more or less compact surface layer, since it would bring about a maximum at ca. 7.5 eV [34,39]. The results are in agreement with XPS: UPS with lower information depth indicates with higher sensitivity the presence of surface impurities (for example, the O 2p peak at ∼4 eV). The less carbon and also the low amount of oxidized metals were not sufficient to suppress the high intensity at the FE in PdPt samples. $H_2$ treatment at 473 K increased the Fermi-edge intensities.

## 4. Conclusions

Nanosized Pd, Pt and PdPt bimetallic particles have been successfully prepared by the reduction of $K_2PdCl_4$ and/or $K_2PtCl_4$ in the presence of cationic surfactant, $C_{14}$TABr. They were characterized by different techniques. The bulk composition and the mean particle size of the catalysts have been determined by EDS and HRTEM. The size of most of the particles was 4–6 nm, except for Pt, showing typical sizes around 14 nm. The monometallic Pd and Pt samples exhibited a more or less hexagonal shape projection. The bimetallic nanoparticles, in turn, seem to have aggregated and exhibited a more irregular, rounded shape. The bulk composition of the bimetallic samples determined by EDS in the "as prepared" state was close to their nominal value, while XPS indicated Pt enrichment near to the surface. The Pt content decreased slightly after treatment in $H_2$ at 473 K. XPS detected carbon impurities in all samples, Pd and Pt retaining more than twice as much carbon as the bimetallic (4:1 and 1:4) particles. The O 1s line (observable with Pt only) showed ca. 15% oxygen, present mainly as surface PtO as well as adsorbed $OH/H_2O$. The comparison of the Pd 3d and Pt 4f lines of the untreated samples with those measured after $H_2$ treatment pointed to the presence of small amounts of oxidized metals in the "as received" state. $H_2$ at 473 K removed most of the

oxygen impurity. The UPS spectra after $H_2$ were closer to those characteristic of pure metals.

## Acknowledgements

The experience of the Department of Colloid Chemistry of the University of Szeged provided the scientific and experimental background of the colloid synthesis. We are grateful for this support, especially to Dr. Zoltán Király. The research was supported partly by the Hungarian National Science Foundation, Grant OTKA T37241. Z.P. thanks for financial support from the Max-Planck-Gesellschaft.

## References

[1] J. Sinfelt, in: G. Ertl, H. Knözinger, J. Weitkamp (Eds.), Handbook of Heterogeneous Catalysis, vol. 4, Verlag Chemie, Weinheim, 1997, p. 1939.
[2] V. Ponec, G.C. Bond, Catalysis by Metals and Alloys, Stud. Surf. Sci. Catal., vol. 95, Elsevier, Amsterdam, 1995.
[3] C.T. Campbell, in: G. Ertl, H. Knözinger, J. Weitkamp (Eds.), Handbook of Heterogenous Catalysis, vol. 2, Wiley-VCH, Weinheim, 1997, p. 814.
[4] J.L. Margitfalvi, I. Borbath, E. Tfirst, A. Tompos, Catal. Today 43 (1998) 29.
[5] F.J. Kuijers, V. Ponec, Appl. Surf. Sci. 2 (1978) 43.
[6] L. Cerveny (Ed.), Catalytic Hydrogenation, Stud. Surf. Sci. Catal., vol. 27, Elsevier, Amsterdam, 1985.
[7] Z. Karpinski, Adv. Catal. 37 (1990) 45.
[8] G. Farkas, E. Sipos, A. Tungler, A. Sárkány, J.L. Figueiredo, J. Mol. Catal. A 170 (2001) 101.
[9] Z. Paál, P. Tétényi, Nature 267 (1977) 234.
[10] W. Juszczyk, D. Lomot, Z. Karpinski, Catal. Lett. 31 (1995) 37.
[11] M. Skotak, Z. Karpinski, Chem. Eng. J. 90 (2002) 89.
[12] B. Török, M. Bartók, Catal. Lett. 27 (1994) 281.
[13] B. Török, Á. Molnár, M. Bartók, Catal. Lett. 33 (1995) 331.
[14] I. Pálinkó, F. Notheisz, J.T. Kiss, M. Bartók, J. Mol. Catal. 77 (1992) 313.
[15] R.M. Navarro, B. Pawelec, J.M. Trejo, R. Mariscal, J.L.G. Fierro, J. Catal. 189 (2000) 184.
[16] S. Eriksson, U. Nylén, S. Rojas, M. Boutonnet, Appl. Catal. A 265 (2004) 207.
[17] Z. Paál, H. Zimmer, J.R. Günter, R. Schlögl, M. Muhler, J. Catal. 119 (1989) 146.
[18] M. Boutonnet, J. Kizling, P. Stenius, G. Maire, Colloids Surf. 5 (1982) 209.
[19] Y. Berkovich, N. Garti, Colloids Surf. 128 (1997) 91.
[20] R. Touroude, P. Girard, G. Maire, J. Kizling, M. Boutonnet-Kizling, P. Stenius, Colloids Surf. 67 (1992) 9.
[21] M.-L. Wu, D.-H. Chen, T.-C. Huang, J. Colloid Interface Sci. 243 (2001) 102.
[22] M. Yashima, L.K.L. Falk, A.E.C. Palmqvist, K. Holmberg, J. Colloid Interface Sci. 268 (2003) 348.
[23] A. Horváth, A. Beck, A. Sárkány, Zs. Koppány, A. Szücs, I. Dékány, Z.E. Horváth, L. Guczi, Solid State Ionics 141–142 (2001) 147.
[24] I. Dékány, L. Turi, E. Tombácz, J. Fendler, Langmuir 11 (1995) 2285.
[25] A. Beck, A. Horváth, A. Szücs, Z. Schay, Z.E. Horváth, Z. Zsoldos, I. Dékány, L. Guczi, Catal. Lett. 65 (2000) 33.
[26] B. Veisz, Z. Király, L. Tóth, B. Pécz, Chem. Mater. 14 (2002) 2882.
[27] F.J. Kuijers, B.M. Tieman, V. Ponec, Surf. Sci. 75 (1978) 657.
[28] A. Szabo, Z. Paál, A. Szász, J. Kojnok, D.J. Fabian, Appl. Surf. Sci. 40 (1989) 77.
[29] L. Fiermans, R. De Gryse, G. De Doncker, P.A. Jacobs, J.A. Martens, J. Catal. 193 (2000) 108.
[30] N. Toshima, Y. Shiriashi, A. Shotsuki, D. Ikenaga, Y. Wang, Eur. Phys. J. D16 (2001) 209.
[31] N. Toshima, M. Harada, T. Yonezawa, K. Kushihashi, K. Asakura, J. Phys. Chem. 95 (1991) 7448.
[32] N. Győrffy, L. Tóth, M. Bartók, J. Ocskó, U. Wild, R. Schlögl, D. Teschner, (Part II), J. Mol. Catal. A, in press.
[33] J. Find, Z. Paál, R. Schlögl, U. Wild, Catal. Lett. 65 (2000) 19.
[34] Z. Paál, U. Wild, A. Wootsch, J. Find, R. Schlögl, Phys. Chem. Chem. Phys. 3 (2001) 2148.
[35] D. Briggs, M.P. Seah (Eds.), Practical Surface Analysis, vol. 1, Wiley, Chichester, 1990, p. 635 (Appendix 6).
[36] B. Veisz, Z. Király, Langmuir 19 (2003) 4817.
[37] Z. Paál, U. Wild, R. Schlögl, Phys. Chem. Chem. Phys. 3 (2001) 4644.
[38] Z. Paál, R. Schlögl, G. Ertl, J. Chem. Soc., Faraday Trans. 88 (1992) 1179.
[39] N.M. Rodriguez, P.E. Anderson, A. Wootsch, U. Wild, R. Schlögl, Z. Paál, J. Catal. 197 (2001) 365.
[40] K. Noack, H. Zbinden, R. Schlögl, Catal. Lett. 4 (1990) 145.
[41] K.S. Kim, N. Winograd, R.E. Davis, J. Am. Chem. Soc. 93 (1971) 6296.